JOURNAL OF APPLIED ELECTROCHEMISTRY **26** (1996) 969–975

Effect of halide ions on electroless nickel plating

G.-S. TZENG

Department of Mathematics & Science Education, National Hualien Teachers College, Hualien, 97055, Taiwan, ROC

Received 2 October 1995; revised 15 January 1996

The effect of halide ions (F^-, Cl^-, Br^-, I^-) on nickel deposition in acidic electroless nickel plating baths is investigated. Halide ions were found to have a significant effect on the nickel deposition and the results could not fully be explained using mixed-potential theory. A correlation between the stability constants of halide ions with palladium (II) ions and the plating rate is proposed to explain the observations. Various parameters, such as the activation energy, deposit microstructure and phosphorus contents of the plating bath in the presence of various halide ions, were also studied.

1. Introduction

The electroless deposition of nickel–phosphorus alloys is widely used in diverse fields, such as the aerospace, automotive, electronics, nuclear, oil and gas production and valve industries [1]. For many applications, the most important properties of these deposits are their high hardness, uniform thickness, remarkable wear and good corrosion resistance. Thus, electroless nickel–phosphorus alloys are being increasingly used as protective layers against wear and corrosion [2–5].

Electroless nickel plating is complicated owing to the autocatalytic nature of the reaction. Several parallel reactions occur during the deposition. The mechanism and kinetics of electroless nickel plating has been studied by many workers [4–11] from chemical and electrochemical viewpoints. Four different reaction mechanisms have been proposed to account for electroless nickel plating. Irrespective of the reaction mechanism, the deposition is believed to be initiated by catalytic dehydrogenation of the reducing agent and it is generally accepted that hydride ion and atomic hydrogen mechanisms occur. The overall reaction can be represented by

$$2\,H_2PO_2^- + 2\,H_2O + Ni^{2+} \xrightarrow[\text{surface}]{\text{catalytic}} Ni + 4H^+ + 2\,HPO_3^{2-} + H_2 \qquad (1)$$

The codeposition reaction of phosphorus in the deposit can also be represented by Equations 2 or 3:

(a) hydride ion mechanism

$$2\,H_2PO_2^- + 2\,H^- \longrightarrow 2\,P + 4\,OH^- + H_2 \qquad (2)$$

(b) atomic hydrogen mechanism

$$4\,H_2PO_2^- \longrightarrow 2\,H_2PO_3^- + H_2 + 2\,P + 2\,OH^- \qquad (3)$$

Mixed-potential theory [12–15] has been proposed to explain electroless metal plating. According to this theory, the cross-over point of the partial anodic and cathodic polarization curves corresponds to the plating potential and plating current. Therefore, the instantaneous rate of electroless nickel deposition can be reliably estimated by the polarization resistance method.

It has been reported [1, 4] that electroless nickel plating baths containing fluoride or chloride ion deposit nickel at higher rate. However, little attention has been focused on establishing the influence of halide ions on the deposition behaviour.

An attempt is made in this work to understand the effects of halide on the plating rate, deposit composition and microstructure, anodic and cathodic polarization resistance and activation energy of electroless Ni–P on copper substrates.

2. Experimental

All solutions were prepared with reagent grade chemicals and deionized water. The bath composition is given in Table 1 except when otherwise specified. The acidity of the different baths was adjusted with H_2SO_4 or NH_4OH solution.

Copper sheets (99.9% pure) of area 9 cm^2 were used as substrate. The surface was cleaned with H_2O_2/H_2SO_4 (20 : 50) solution and activated in palladium chloride (1 g dm^{-3} $PdCl_2$ plus 1 cm^3 dm^{-3} HCl) solution for 5 s [1]. The sample was then weighed and immersed in 125 cm^3 of plating solution for 20 min at specified temperature; the temperature was controlled by circulating thermostatted water through the double wall of the cell. After plating, the deposits were washed with distilled water, dried and reweighed. The plating rates were determined as weight gained in mg h^{-1} cm^{-2} [16] at pH 4.6, pH 5.0 or pH 5.5.

The phosphorus contents in the deposit were determined by energy dispersive X-ray spectrometry (EDXS, Jeol JSM-840A) linked with a scanning electron microscope; the morphology was also examined.

Polarization experiments were carried out on platinum foil (0.8 cm^2) using an electrochemical interface system (Schlumberger S1-1286) equipped with a microcomputer interface. Data were transferred to a

0021-891X © 1996 Chapman & Hall

Table 1. Composition of plating bath with concentrations (M)

Constituent	*Bath A*	*Bath B*	*Bath C*	*Bath D*	*Bath E*
$NiSO_4$	0.1	0.1	0.1	0.1	0.1
NaH_2PO_2	0.25	0.25	0.25	0.25	0.25
CH_3COONH_4	0.13	0.13	0.13	0.13	0.13
NaF		0.1			
NaCl			0.1		
NaBr				0.1	
NaI					0.1

microcomputer for storage and analysis. Platinum wire and saturated calomel electrodes (SCE) were used as counter and reference, respectively.

The concentration used in the polarization measurements was the same as in the plating rate experiments (Table 1). The experiment was carried out at room temperature and oxygen was purged by bubbling nitrogen through the solution prior to the experiment.

The anodic polarization curves were derived from the hypophosphite-reduced electroless nickel bath in the absence of metal ions and the cathodic polarization curves were derived from the hypophosphite-reduced electroless nickel bath in the absence of hypophosphite. The scan rate was 5 mV s^{-1} for all measurements.

3. Results and discussion

3.1. *Plating rate study*

For baths A to E, the concentration of free NH_3 in the plating bath was found to be very low under our experimental conditions (pH 4.6, 5.0 or 5.5) and halide ion did not coordinate with nickel ion [17]. Therefore, the nickel ion in each bath (A to E) was virtually noncomplexed. Although many workers [4, 5, 7] report that complexing agents are necessary to increase solution stability, the present observation shows each bath was stable during the deposition.

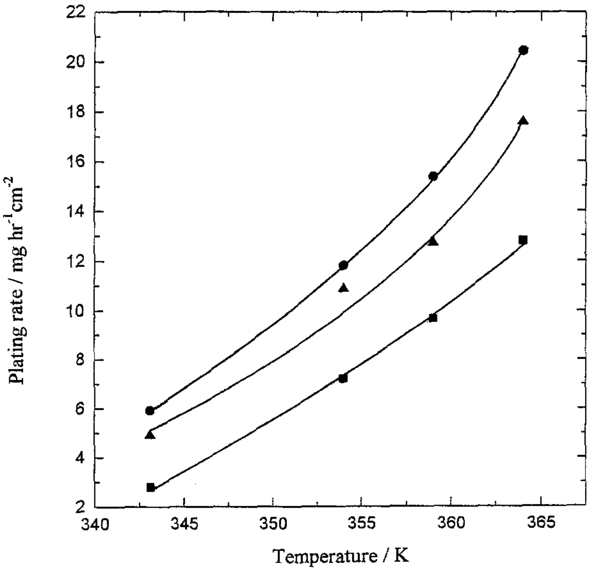

Fig. 1. Effects of temperature and pH on plating rate of bath A. Key: (●) pH 5.5; (▲) pH 5.0; (■) pH 4.6.

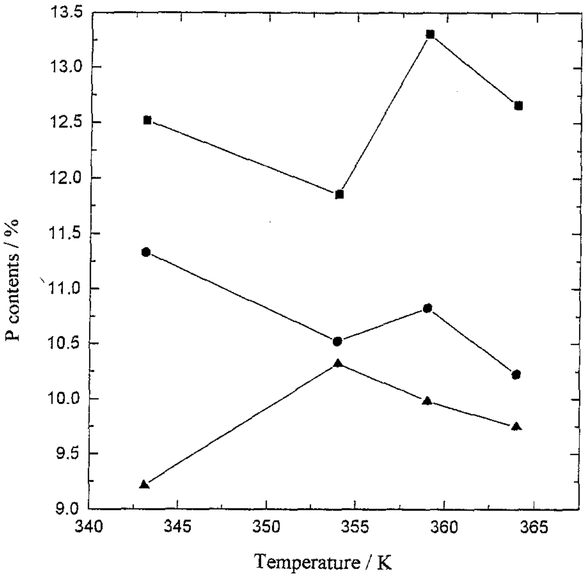

Fig. 2. Effects of temperature and pH on phosphorus content of deposit of bath A. Key: (■) pH 4.6; (●) pH 5.0; (▲) pH 5.5.

The plating rates for bath A, at different temperatures and pH, are shown in Fig. 1. Although the nickel ion was nearly noncomplexed, under identical pH conditions (pH 4.6, 5.0 or 5.5), the plating rate of bath A increased sharply with temperature. For example, at pH 5.0, the plating rate at 343 K was 4.9 mg h^{-1} cm^{-2}, but the rate increased to 17.6 mg h^{-1} cm^{-2} at 364 K. In addition, the plating rate of bath A also increased with pH at the same temperature. These results can be explained using the Arrhenius relationship and Equation 1. Similar trends have also been observed previously [4].

Figure 2 shows the deposit phosphorus content from bath A at different temperatures and pH. It can be seen that at a fixed temperature, the higher the solution pH, the lower the phosphorus content in the deposit. For example, at 359 K, the weight percent of phosphorus in the deposit at pH 4.6 was about 13%, but at pH 5.5 it decreased to about 10%. From reaction stoichiometry, this phenomenon may be explained by Equations 2 or 3. In addition, the distribution of phosphorus content was random for bath A at any pH value (Fig. 2). Kalantary *et al.* [18] had reported that the nickel deposit is generally found to contain 3–15% codeposited phosphorus from the hypophosphite ion system. The results obtained in Fig. 2 are consistent with those results.

The effect of halide ion (0.1 M) on the plating rate at different temperatures for baths B, C, D and E are shown in Fig. 3. The plating rates for baths B and C, which are similar to bath A, increased sharply with increase in temperature. Previously it has been reported that electroless plating solution containing fluoride or chloride ion increases the nickel plating rate, but the present results are in contradiction [1, 4]. However, it is found that the plating rate is less influenced by chloride ion. Hence, nickel sulfate is

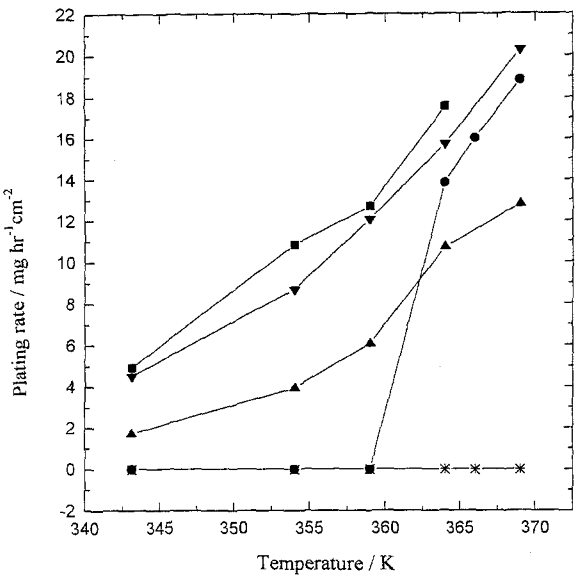

Fig. 3. Effects of halide ($X^- = 0.1$ M) and temperature on plating rate of baths A, B, C, D and E at pH 5.0. Baths: (■) A; (▲) B; (▼) C; (●) D; (∗) E.

usually used as a nickel source in electroless nickel plating. The plating rate from the bromide ion bath (bath D) could not be estimated until the temperature of the bath reached 364 K (Fig. 3). The incubation time (364 K, about 10 min) of bath D was about five times larger than that for baths A, B or C. It can be seen from Fig. 3 that the iodide ion bath (bath E) does not deposit, no matter how long the incubation time. The differential effect of the halide ion on the plating rate will be discussed later.

The effect of temperature on the plating rate was studied and the ln(rate) against $1/T$ relationship is given in Fig. 4. The activation energy (E) for the deposition was calculated from the slope of the ln(rate) against $1/T$ plot, using the method of least squares. The activation energy for different baths at various conditions are given in Table 2.

Table 2. Activation energy of plating bath

Bath	*Condition, pH*	E/kJ mol^{-1}
A	4.6	76.6
	5.0	62.7
	5.5	61.9
B	5.0	85.8
C	5.0	63.2
D	5.0	69.0

Although the temperature range was too narrow to calculate the activation energy accurately, the activation energy of bath D was estimated and found to be about 69.0 kJ mol^{-1}. For bath E, as deposition did not occur, the activation energy was very high. Therefore, under the same experimental conditions, the order of activation energy of the various baths was: bath E (I^-) > bath B (F^-) > bath D (Br^-) > bath C (Cl^-) > bath A (no halide ion).

The halide ion effect on the phosphorus content is shown in Fig. 5. The difference among the phosphorus contents of baths A, C and D were very small. However, bath B, under the same experimental conditions, has a higher phosphorus content than that of the other baths.

The halide ion has a significant effect on the plating rate (Fig. 4). The concentration effect of fluoride or chloride on the plating rate was also investigated (Fig. 6). The plating rate of bath C was nearly constant (about 9 mg h^{-1} cm^{-2}) when the concentration of chloride ion was above 0.01 M, but the plating rate of bath B significantly decreased when the fluoride ion concentration increased.

3.2. *Polarization study*

The polarization curves for various baths for the anodic oxidation of hypophosphite and the cathodic

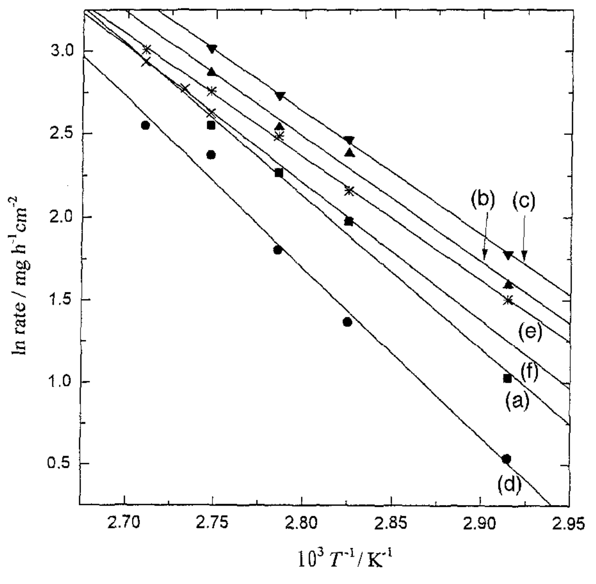

Fig. 4. Determination of activation energy. Baths: (a) A, pH 4.6; (b) A, pH 5.0; (c) A, pH 5.5; (d) B; (e) C; (f) D.

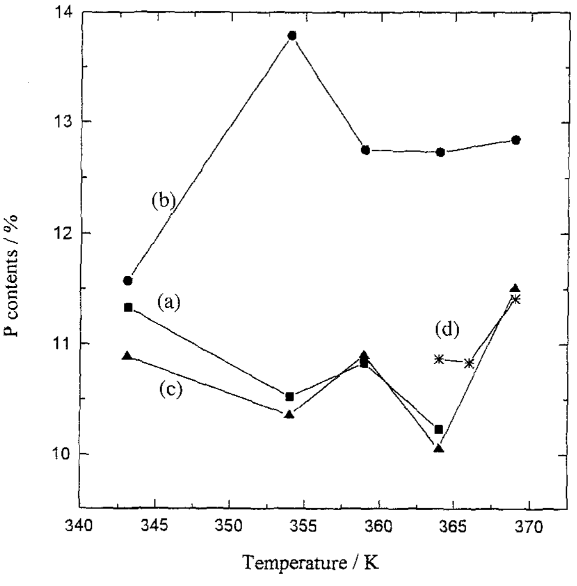

Fig. 5. Effects of halide ion and temperature on phosphorus contents of deposit of bath A, B, C and E at pH 5.0. Baths: (a) A; (b) B; (c) C; (d) D.

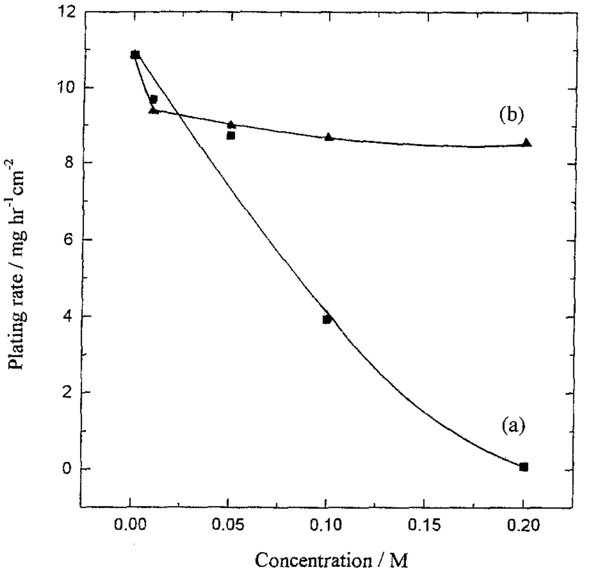

Fig. 6. Effect of halide ion concentration on plating rate of baths B and C at pH 5.0 and temperature 80 °C. Baths: (a) A and (b) C.

reduction of nickel ion on the platinum electrode are shown in Fig. 7 (a)–(e). If the reaction follows mixed-potential theory, the potential and current at the intersections of the anodic and cathodic polarization curves should correspond to the plating potential and plating current, respectively.

Figure 7 (a)–(d) shows that the plating potentials of baths A, B, C and D are nearly equal and are about 0.15 V vs SCE. However, the anodic and cathodic polarization curves of bath E did not intersect (Fig. 7(e)) and plating did not proceed; these results are consistent with those of the plating experiment. Fig. 7 (a)–(e) also shows that the order of the plating current in the electroless nickel plating is: bath A (no halide ion, 10^{-4} A) $\approx$ bath B (F^-, 10^{-4} A) $>$ bath C (Cl^-, 5×10^{-5} A) $>$ bath D (Br^-, 1.5×10^{-5} A) $>$ bath E (I^-, 0 A).

According to mixed-potential theory, the order of plating rate of electroless nickel deposit should be consistent with the sequence of plating currents, and it is interesting to find that, except for bath B, the sequence was fully consistent with the experimental observation (Fig. 3). Evidently, the mixed-potential theory cannot fully explain the electroless nickel plating mechanism and it is possible that other factors affect the deposition rate.

3.3. *Plating mechanism*

The principle redox reactions in the bath are the reduction of nickel ion to nickel metal and the oxidation of hypophosphite ion to phosphite. Because the initial reaction can only take place at activated palladium nuclei, dehydrogenation of the reductant is proposed as the first step [6] and the overall reaction can be represented by Equation 1:

$$2\,H_2PO_2^- + 2\,H_2O + Ni^{2+} \xrightarrow[\text{surface}]{\text{catalytic}} Ni + 4H^+ + 2\,HPO_3^{2-} + H_2 \qquad (1)$$

Table 3. The stability constants (k) of Pd^{2+} and Ni^{2+} with halide ion

Halide ion	*Log k* (*with Pd^{2+}, $I = 0.1$ M*)	*Log k* (*with Ni^{2+}, $I = 2.0$ M*)
F^-	*	*
Cl^-	ML (4.47) ML_2 (7.74) ML_3 (10.2) ML_4 (11.5)	ML (−0.21)
Br^-	ML (5.17) ML_2 (9.42) ML_3 (12.7) ML_4 (14.9)	ML (−0.12)
I^-	ML_4 (24.5)	*

* Stability constant could not be found in the literature.

If additives such as the anion, stabilizer, complexing agent, accelerator and others are added to the bath, they show strong adsorption on the metal surface and block surface active sites that are required for electrocatalysis. As a result, the plating rate (Equation 1) decreases or ceases [19].

Conway *et al.* [20] reported that if the anion can coordinate with the metal ion, the larger the stability constant, the more anions can adsorb on the surface. The stability constants of halide with palladium (ii) ion or nickel ion at 25 °C are given in Table 3 [17].

Table 3 shows that the stability constants of halide with nickel ion can be neglected compared with the stability constants of palladium (ii) ion. The order of stability constants of halide with palladium (ii) ion is $MI_4 > MBr_4 > MCl_4$. Therefore, according to Conway *et al.*, the order of halide ion absorption on activated palladium nuclei should follow the sequence: $I^- > Br^- > Cl^-$.

The increasing number of halide ions adsorbed on the activated palladium nuclei increases the number of ions blocking the surface active sites that are required for electrocatalysis, resulting in slowing down or cessation of the plating rate (Equation 1). Hence, under the same conditions, the plating rate (Fig. 3) for various baths follows the sequence: bath A (no halide ion) $>$ bath C (Cl^-) $>$ bath D (Br^-) $>$ bath E (I^-). Evidently, the activation energies of the various baths were in the reverse order of plating rate.

The stability constants of fluoride ion with palladium (ii) ion could not be found [17] but can be predicted from an empirical formula [21]:

$$\log Q = -1.56 + 0.48\, Z_+^2/r_+ \qquad (4)$$

where Q is the stability constant for the reaction

$$Pd^{2+} + F^- \longrightarrow PdF^- \qquad (5)$$

and $Z_+(+2)$ and r_+ (80 pm) [22] are the charge and radius of the palladium (ii) ion, respectively. The predicted stability constant of fluoride with the palladium (ii) ion is smaller than that of other halide ions. Thus, the work of Conway *et al.* can not explain the rate from the bath containing fluoride ion (bath B). This

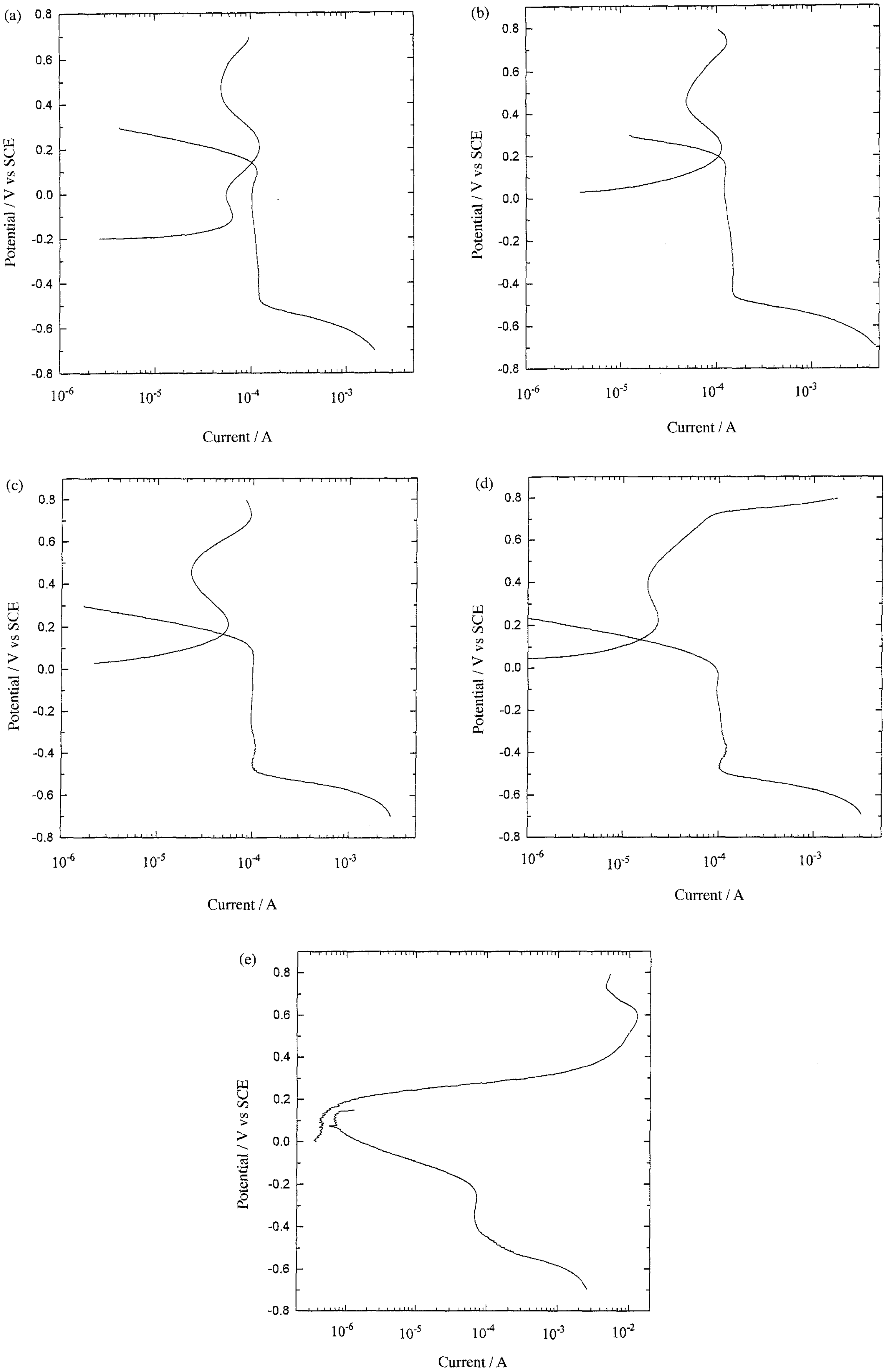

Fig. 7. Anodic and cathodic polarization on a platinum electrode in electroless nickel plating baths in the absence of either Ni^{2+} or $H_2PO_2^-$. Baths (a) A; (b) B; (c) C; (d) D; (e) E.

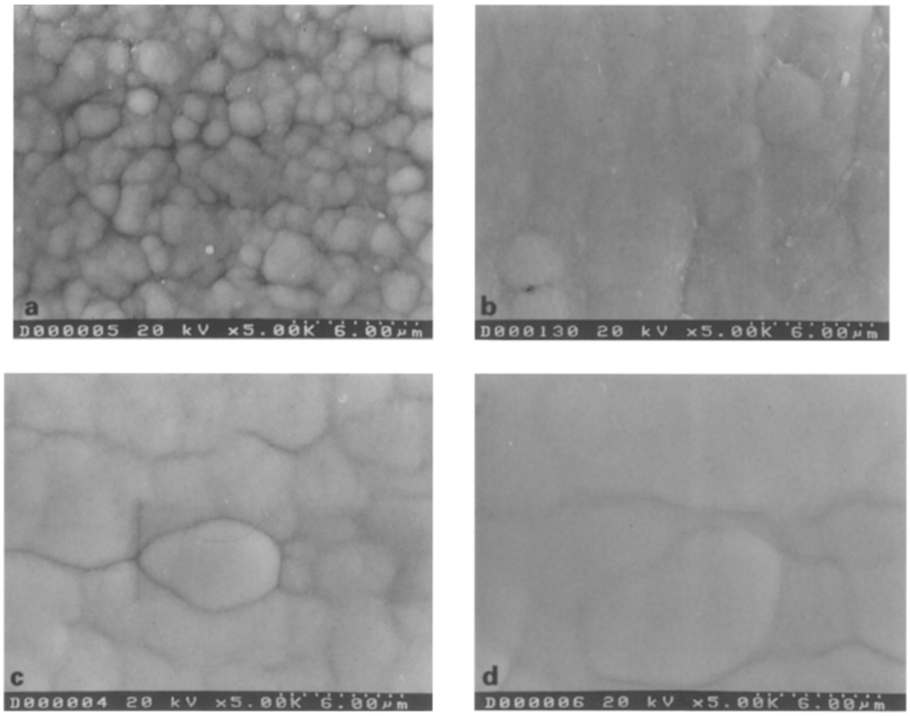

Fig. 8. Effect of temperature on microstructure of electroless nickel deposits from bath A at pH 5.0. Temperatures: (a) 343 K; (b) 354 K; (c) 359 K; (d) 364 K.

phenomenon may be explained by the fact that fluoride ion, which has a small size and high charge, becomes a larger hydrated ion in the aqueous plating bath. This hydrated ion may block the activated palladium nuclei, resulting in a decrease in the plating rate; the larger the concentration of fluoride ion, the greater the decrease in plating rate.

3.4. *Surface morphology study*

Figures 8 (a)–(d) and 9(a)–(d) show scanning electron micrographs of nickel deposits obtained from bath A at pH 5.0 and pH 5.5, respectively. Although other workers [4, 5] report that electroless nickel deposits are amorphous, the present observation shows that

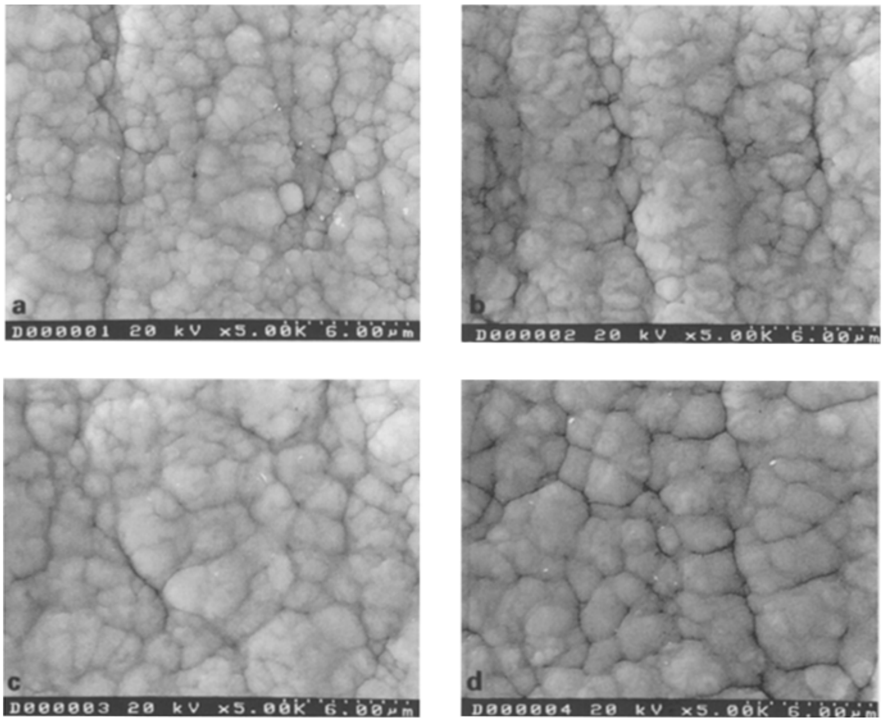

Fig. 9. Effect of temperature on microstructure of electroless nickel deposits from bath A at pH 5.5. Temperatures: (a) 343 K; (b) 354 K; (c) 359 K; (d) 364 K.

the grain size is clearly determined. At pH 5.5, the grain size is less influenced by temperature; than at pH 5.0 where temperature has a more significant effect.

Under the same plating conditions, the scanning electron micrographs of the deposits from the fluoride containing (bath B) or chloride containing (bath C) are similar to Fig. 8. This shows that fluoride and chloride ion does not have a significant effect on the morphology of the deposit.

4. Conclusion

The effect of halide ion on electroless nickel plating was investigated and following conclusions were drawn:

(i) Under the same plating conditions, the order of plating rate for various baths follows the sequence: bath A (no halide ion) > bath C (Cl^-) > bath D (Br^-) > bath B (F^-) > bath E (I^-). The activation energy for various baths follows the reverse order.

(ii) Under the same experimental conditions, the deposits obtained from the fluoride ion bath have a higher phosphorus content than those from other baths.

(iii) Mixed-potential theory does not fully explain the plating rate from various halide ion baths. The adsorption of halide ion on activated palladium nuclei must therefore be considered. Except for the fluoride ion bath, the relationship of plating rate with stability constant of halide with palladium (II) ion was established. It was experimentally observed that the larger the stability constants of halide with palladium (II) ion, the smaller is the plating rate.

(iv) Fluoride and chloride ions did not have a significant effect on the microstructure of the deposits.

References

[1] T. Mimani and S. M. Mayanna, *Plat. Surf. Finish* **80**(2) (1993) 66.
[2] N. Kanani, *Trans. Inst. Metal Finish.* **70**(1) (1991) 14.
[3] K. Parker, *Plat. Surf. Finish.* **79**(3) (1992) 29.
[4] F. A. Lowenheim, 'Electroplating', McGraw-Hill, New York (1978) part 3, pp. 391–403.
[5] C. R. Shipley Jr, *Plat. Surf. Finish* **71**(6) (1984) 92.
[6] J. E. A. M. Van Den Meerakker, *J. Appl. Electrochem.* **11** (1981) 395.
[7] I. Ohno, *Mater. Sci. Eng. A* **146** (1991) 33.
[8] A. W. Goldenstein, W. Rostoker and F. Schossberger, *J. Electrochem. Soc.* **104** (1957) 104.
[9] L. F. Spencer, *Metal Finish.* **72** (1974) 35.
[10] S. F. Smith, *ibid.* **77**(5) (1979) 60.
[11] L. M. Abrantes and J. P. Correia, *J. Electrochem. Soc.* **141** (1994) 2356.
[12] M. Stern and A. L. Geary, *ibid.* **104** (1957) 56.
[13] M. Paunovic, *Plating* **55** (1968) 1161.
[14] Y. Okinaka, *J. Electrochem. Soc.* **120** (1973) 739.
[15] I. Ohno and S. Haruyama, *Surf. Technol.* **13** (1981) 1.
[16] A. Hung and K. M. Chen, *J. Electrochem. Soc.* **136** (1989) 72.
[17] R. M. Smith and A. E. Martell, 'Critical Stability Constants', vol. 4, Plenum Press, New York (1976) pp. 96–126.
[18] M. R. Kalantary, K. A. Holbrook and P. B. Wells, *Trans. Inst. Metal Finish.* **71**(2) (1993) 55.
[19] A. M. T. van der Putten and J. W. G. de Bakker, *J. Electrochem. Soc.* **140** (1993) 2229.
[20] B. E. Conway, J. O'M Bockris, E. Yeager, S. U. M. Khan and R. E. White, 'Comprehensive Treatise of Electrochemistry', vol. 7, Plenum Press, New York (1983) pp. 521–22.
[21] F. A. Cotton and G. Wilkinson, 'Advanced Inorganic Chemistry', 3rd edn, J. Wiley & Sons, New York (1972) pp. 471–72.
[22] D. R. Lide, 'Handbook of Chemistry and Physics' 72nd edn, CRC Press, (1991) pp. 12–18.